Precise force measurement method by a Y-shaped cavity dual-frequency laser

Guangzong Xiao (肖光宗)*, Xingwu Long (龙兴武), Bin Zhang (张 斌), and Geng Li (李 耿),

Department of Optoelectronic Engineering, College of Optoelectronic Science and Engineering, National University of Defense Technology, Changsha 410073, China

**Corresponding author: xiaoguangzong@163.com*

Received January 18, 2011; accepted May 9, 2011; posted online July 11, 2011

A novel precise force measurement based on a Y-shaped cavity dual-frequency laser is proposed. The principle of force measurement with this method is analyzed, and the analytic relation expression between the input force and the change in the output beat frequency is derived. Experiments using a 632.8-nm Y-shaped cavity He-Ne dual-frequency laser are then performed; they demonstrate that the force measurement is proportional to a high degree over almost five decades of input signal range. The maximum scale factor is observed as 5.02×10^9 Hz/N, with beat frequency instability equivalent resolution of 10^{-5} N. By optimizing the optical and geometrical parameters of the laser sensor, a force measurement resolution of 10^{-6} N could be expected.

OCIS codes: 120.4640, 120.5475, 140.1340, 140.3140

doi: 10.3788/COL201109.101201.

Precise measurement of force and force-related magnitudes, such as acceleration, pressure, and mass, is an often demanded task in modern engineering and science[1−3]. In recent decades, some research efforts have been intensified to utilize optical measurement procedures for obtaining precise force measurement.

In most previous attempts to apply the optical effect for force measurement, the intensity, polarization state, or phase of the transmitted light was often modulated by the input force. They are commonly called "passive optical force sensor", examples of which are the optical fiber micro electro mechanical system (MEMS) force sensors[4,5] and the optical fiber Bragg grating force sensor[6]. The optical fiber elastic deformation effect in interferometers was also used to carry out force measurement by modulating the phase of the transmitted light[7−9]. In addition, the silicon-on-insulator MEMS (SOI-MEMS) technology used in force sensors is now being widely studied[10]. However, these methods and technology always result in nonlinear characteristics, which is important to the precious measurement.

Compared with the passive optical force sensor, active optical force sensor, another optical measurement technique is more promising. This technique enables the modulation of the laser frequency to be strictly proportional to the input force, which has been a persisting issue for decades now.

One type of active optical force sensor that has been widely researched about is the one that utilizes the laser crystal's photoelastic effect, such as Nd:YAG. In 1989, Holzapfel *et al.* carried out a force-to-frequency conversion using the photoelastic effect inside a He-Ne laser cavity[11.12]. They demonstrated that precise conversion of force to frequency can be achieved by applying the resonator-internal photoelastic effect. In 1993, they developed the force measurement based on the photoelastic effect in solid-state lasers[13]. In 2000, utilizing the same principle, they achieved a very large measurement range of nine decades and a strictly proportional conversion of force into frequency for modulating frequencies starting from DC up to at least 100 kHz[14]. Meanwhile, Zhang *et al.* realized the determination of internal stress in Nd:YAG crystal by applying the laser frequency splitting method with high resolution of 5 Pa. Its resolution is approximately five to eight orders of magnitude higher than those of conventional methods[15]. They also used an all-optical pressure sensor and achieved a sensitivity of 1.31 MHz/kPa[16].

In this letter, another active optical force sensor based on the press-refractivity effect of gas is presented. The key basis of this sensor is a Y-shaped cavity dual-frequency laser. The laser's basic principle and structure, as well as the force sensor's basic principle, signal transforming procedures, and mathematical modeling are described. The primary experimental study and its setup are reported. The experimental results are discussed and analyzed.

The main design features of the force sensor in this study are shown in Fig. 1. Force-to-frequency conversion is carried out by means of a Y-shaped cavity dual-frequency laser (Fig. 2) and a gas sylphon of special structure[17].

For convenience, we specify two terms used in this letter. P-light means that the electric field vector is perpendicular to the plane of incidence, while S-light means that the electric field vector is parallel to the plane of

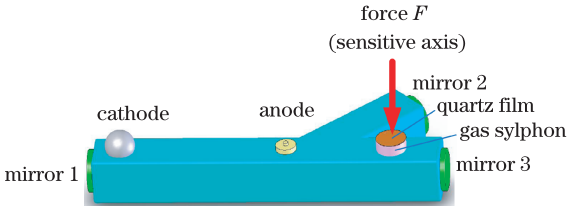

Fig. 1. Force transducer by a Y-shaped cavity dual-frequency laser.

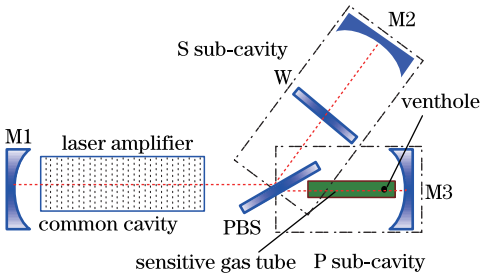

Fig. 2. Y-shaped cavity dual-frequency laser.

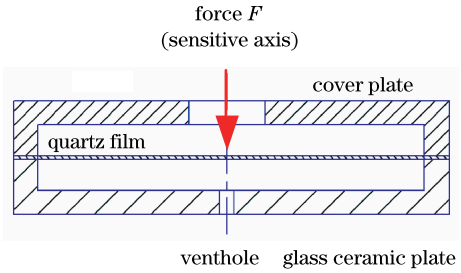

Fig. 3. The gas sylphon's cutaway view.

incidence. A Y-shaped cavity dual-frequency laser is a novel dual-frequency laser based on the Y-shaped cavity frequency splitting method. The laser amplifier, in which both the S-light and P-light pass through, provides gain for them. The portion of the cavity formed with mirror 1 and the polarization beam splitter (PBS) is called the "common cavity". The S-light and the P-light are separated from each other by the PBS and then pass through the different sub-cavities. M1 is the output plane mirror with reflectance of 99.7%. Meanwhile, M2 and M3 are highly reflective spherical mirrors with reflectance of 99.9% and curvature radius of 2 m. The sub-cavity formed with the PBS and M2 is called "S sub-cavity", while that formed with the PBS and M3 is called "P sub-cavity". The common cavity joined with the S sub-cavity and the P sub-cavity is called the "Y-shaped cavity" in view of its shape. W is an anti-reflective window, which is a crystal glass substrate coated by anti-reflective film.

The key element of the Y-shaped cavity dual-frequency laser is the PBS, whose reflectance for S-light and transmittance for P-light are both 99.9% at the specific angle of incidence due to its specially designed film structure and deposition process of optical coatings. In such case, the laser oscillator is excited in two longitudinal modes, which are polarized linearly and orthogonally to each other. According to the principle of laser, the frequencies for S-light $v_{\rm s}$ and P-light $v_{\rm p}$ can respectively be written as

$$\nu_{\rm s} = s \cdot \frac{c}{2\,(l_{\rm c} + l_{\rm s})}, \quad \nu_{\rm p} = p \cdot \frac{c}{2\,(l_{\rm c} + l_{\rm p})}, \tag{1}$$

where $l_{\rm c}$ is the optical length of the common cavity; $l_{\rm p}$ is the optical length of the P sub-cavity; $l_{\rm s}$ is the optical length of the S sub-cavity; and s and p are natural numbers.

As shown in Fig. 3, the gas sylphon is composed of the quartz film, glass ceramic plate, and sensitive gas. The super-thin quartz film is conglutinated with the glass ceramic plate to form an airtight room, which is filled with sensitive gas such as air of a certain pressure. There is a cover plate on the gas sylphon in order to minimize the influence of environmental factors, including temperature and environmental pressure. The venthole of the gas sylphon is connected to the sensitive gas tube in the P sub-cavity of the laser (Fig. 2).

The gas sylphon is used to produce the changes in the P sub-cavity's optical path length induced by the input force. When the force F is acted on the center of the quartz film along the sensitive axis as shown in Fig. 1, it will induce a change in the sensitive gas' refractive index Δn, given by[17]

$$\Delta n = \frac{5}{128} \frac{k\rho R^4}{V_0 D\,(1+\eta)} \cdot F, \tag{2}$$

where k and ρ are the sensitive gas' Gladstone-Dale constant and density, respectively; D is the quartz film's bending rigidity; R is the glass ceramic plate's radius; V_0 is the sensitive gas' initial total volume including the cubages of the gas sylphon and sensitive gas tube, depending on the glass ceramic plate's radius R and height ε; $\eta = 5/64 \cdot P_0 R^6 D^{-1} V_0^{-1}$ is the correction factor of Δn taking account the gas press' change when the input force is applied on the gas sylphon, which depends on the V_0, D, R, and the sensitive gas' initial pressure P_0. Because of this, the P sub-cavity's optical path is changed, causing a change in the two sub-cavities' optical path length difference. According to Eqs. (1) and (2), the change in the beat frequency Δv between the S-light and the P-light can be written as

$$\delta\,(\Delta v) = v_0 \frac{l_{\rm t}}{n_1 l_{\rm s} + n_0 l_{\rm c}} \cdot \Delta n = E \cdot F. \tag{3}$$

Equation 3 shows the nominal part being exactly proportional to the applied force F, where v_0 is the optical frequency, $l_{\rm t}$ is the length of the sensitive gas tube, and n_0 and n_1 are the refractive indexes of the active gas and sensitive gas, respectively. From Eq. 3, it is known that the nominal scale factor E is constant in relation to the parameters of the laser and gas sylphon.

The experimental scheme as shown in Fig. 4 was used to investigate the principle properties of the new force measurement technique. The experimental setup is composed of three units.

(i) A force transducer – it included a Y-shaped cavity

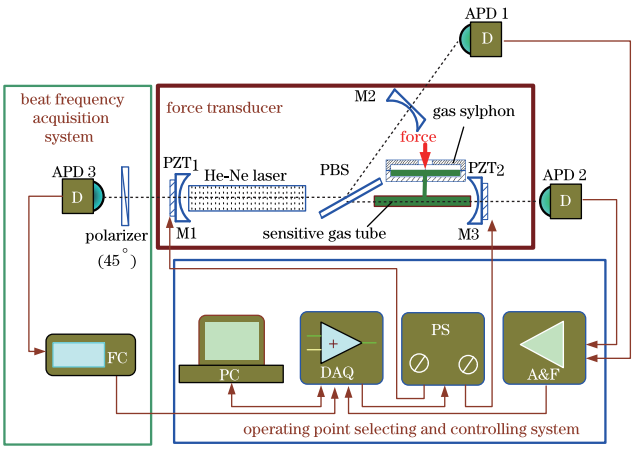

Fig. 4. Experimental setup.

He-Ne dual-frequency laser and a gas sylphon, which are both made of glass ceramic called zero expansion coefficient glass. The common cavity length of the laser l_c= 100 mm, while the two sub-cavities' length $l_p = l_s$ = 20 mm. The length of the sensitive gas tube was about equal to the P sub-cavity's length (Fig. 2). Our experiments were carried out using the gas sylphons of different radii R. The other parameters of the experimental setup were the same as that of a quartz film: t= 0.1 mm; glass ceramic plate: ε = 0.5 mm; and sensitive gas: air with 1 standard atmosphere pressure.

(ii) A selecting and controlling system of operating point – it included two avalanche photo diodes (APDs), two piezoelectric transducers (PZT), an amplifier and filter (A&F), a PZT power supply (PS), a data acquisition circuit (DAQ), and a computer (PC).

(iii) A beat frequency acquisition system – it included an APD, a frequency counter (FC, Agilent 53131A), and a PC.

Precisely defined input signals were produced with different calibrated test masses m_i. With constant acceleration due to earth gravity ($g \approx 9.8$ m·s^{-2}), the different forces $F_i = m_i g$ acting on the quartz film of the gas sylphon were produced. The beams emerging from M2 and M3 provided the operating point (i.e., the longitudinal modes' relative position in the free spectral range of laser) selecting and controlling channel. Their intensities were transformed into electrical signal by APD 1 and APD 2, and then amplified and converted from analog signals into digital signals by A&F and DAQ. A simple but effective method of operating point controlling, based on a comparison of two mode intensities, was applied to keep the laser operating stably through the PZT_1 and PS. Using this method, the center of the two longitudinal modes was selected and controlled at the center frequency of the laser transition. Radiation, emerging from M1, passed through a polarizer and was detected by APD 3. The force-dependent change in the beat frequency Δv between the S-light and the P-light $\delta(\Delta v)$ was then measured by means of the frequency counter (Agilent 53131A). All the measurement processes above were controlled and harmonized mostly by the software in the computer.

The dependence of the beat frequency Δv on the input signal F was investigated experimentally for the gas geometry parameters. A slight sylphons of different increase in the beat frequency Δv was observed for the sudden changes in input signal caused by placing the mass on the quartz film of the gas sylphon. After the removal of the mass, the beat frequency dropped back to its previous value. A series of frequency rises and drops of the same magnitude occurred when the same mass of 984 mg was put and removed as shown in Fig. 5, indicating that this reaction is reproducible. From the constant parts of the measured time, it is concluded that this test process was in operation with good static characteristic. The maximal rise time of about 100 μs was observed when the sample time was 50 μs; hence, we conclude that the dynamic bandwidth of our measurement setup is of the order of kilohertz. Further dynamic characteristic test and analysis are on the horizon. In Fig. 5, the occasionally observed beat frequency peaks at the beginning and the end of each stress interval can be explained by

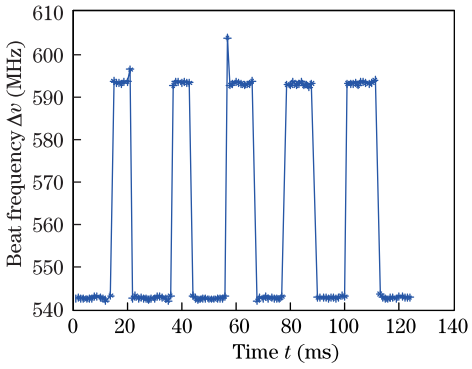

Fig. 5. Time trace of the beat frequency caused by a series of input step masses, mass step m = 983.8 mg, and equivalent force F = 0.0096 N; geometry parameters of the quartz film and glass ceramic plate: R=20 mm, t=0.1 mm, and ε =0.5 mm setup.

the necessary manipulation of taking the mass on and off.

From a sequence of the above-described load test with different test masses, the change in the beat frequency at the well-known constant earth gravity g was ascertained as a function of the test mass weight. The increase in the experimental sensitivity (i.e., scale factor) had been realized in accordance with Eq. (3) by changing the diameter of the gas sylphon. The static characteristics for the three measurement experiments with scale factors E_1=2.24×10^9 Hz/N, E_2=3.12×10^9 Hz/N, and E_3= 5.02×10^9 Hz/N are shown in Fig. 6, with the values of the three scale factors obtained from the experimental data. The diameters of the gas sylphons corresponding to the three different scale factors (i.e., E_1, E_2, and E_3) were 25, 30, and 40 mm, respectively. According to Eq. (3), the nominal scale factors were calculated as $\widetilde{E}_1$ = 2.25×10^9 Hz/N, $\widetilde{E}_2$ = 3.15×10^9 Hz/N, and $\widetilde{E}_3$ = 5.06×10^9 Hz/N. They were mostly in good agreement with the experimental value when taking the manipulation error in to account. The relationship formulas between the changes in the beat frequency Δv and the applied force F can respectively be written as $[\delta(\Delta v)]_1$= (2.24×10^9·F–1.68×10^3) Hz/N, $[\delta(\Delta v)]_2$= (3.12×10^9·F– 1.32×10^3) Hz/N, and $[\delta(\Delta v)]_3$=(5.01×10^9·F–4.63×10^2) Hz/N through data fitting. The fitting residual errors

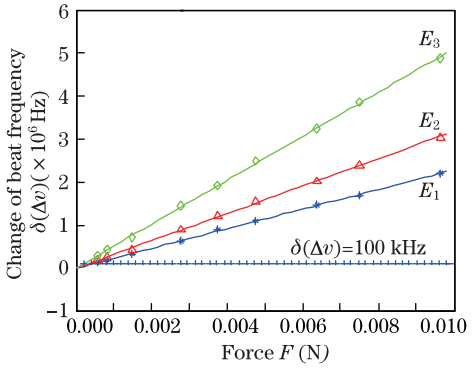

Fig. 6. Static characteristics of the laser force transducer. Different scale factors E_1, E_2, and E_3 are obtained by changing the diameter of the gas sylphon: ∗: E_1=2.24×10^9 Hz/N, R_1 = 25 mm; Δ: E_2=3.12×10^9 Hz/N, R_2=30 mm; ♢: E_3= 5.02×10^9 Hz/N, R_3=40 mm; + is the stability of the beat frequency in a short time (about 10 minutes).

were $delta_1 = 1.67\times10^3$ Hz, $delta_2 = 2.55\times10^3$ Hz, and $delta_3 = 3.60\times10^3$ Hz, respectively. The fitting curves and the experimental data points in Fig. 6 indicate that the system has a good linearity. All the experimental results were taken after having reached the thermal stability of the laser transducer.

A novel force measurement system covering an input range of five decades with a resolution of 10^{-5} N has been demonstrated based on a Y-shaped cavity dual-frequency laser.

The upper measurement limit of the input force is determined by the laser's lasing bandwidth and the scale factor. The low measurement limit is only determined by the resolution, depending on the scale factor and the stability of the beat frequency Δv. In our experiment, the highest scale factor is $E_3=5.02\times10^9$ Hz/N and the longitudinal mode spacing is about 900 MHz, with the upper measurement limit recorded at approximately $F_{\max}=0.18$ N. During the experiment, the observed short-time (about 10 minutes) beat frequency instability was 100 kHz; therefore, the resolution is about 10^{-5} N.

The increase in scale factor can be achieved easily by enlarging the diameter of the gas sylphon or by using the sensitive gas high-refractive index. However, for the constant lasing bandwidth, the upper measurement limit will decrease with the increase in the scale factor. In all, it only enhances the stability of the beat frequency, which ensures good performances of the resolution and the upper and low measurement limits.

The preliminary performance of the upper and low measurement limits still has its flaws due to the beat frequency instability of the laser. The main disturbance of the beat frequency comes from the variation of the difference of the two sub-cavities' length due to thermal expansion. In the laser, the substrate of the PBS is made of crystal glass, whose expansion coefficient is $2\times10^{-7}/^\circ$C. This will lead to the P sub-cavity length's thermal change of 4×10^{-10} m/°C, which is equivalent to 1.25×10^6 Hz/°C. In our experiment, the observed short-time beat frequency instability was mainly attributed to the crystal glass substrate of the PBS. To compensate for such, further effort will be made to place a crystal glass substrate (W) of the same thickness as the PBS coated by the anti-reflective film in the S sub-cavity. In such case, we believe that the thermal disturbance to the beat frequency will be reduced remarkably because it will have little thermal difference when it is very near and with the same thickness.

Other factors affect the performance of the force measurement system. Firstly, the pushing and pulling effects of the laser affect the linearity of the relation between the change in the beat frequency and the change in the difference of the two sub-cavities' optical path length, which is calculated to be about 10^{-5}. This value is small, thus it can be ignored at present. Secondly, the frequency difference lock-in phenomenon leads to the reduction of the force measurement range. Nevertheless, the laser's lock-in phenomenon can be reduced and even eliminated by means of a transverse magnetic field[18].

In conclusion, compared with other laser transducers, this type of laser sensor has some advantages such as having operation stability and versatility. In virtue of the sensitive gas in one sub-cavity being the first step sensor in the laser transducer, the input signals do not disturb the direction of the ray, thereby preventing the operation of the laser to be affected. Furthermore, we conclude that this new laser sensor has a better potential perspective for extensive applications. With the development of an appropriate mechanical structure, it can be applied in the field of electronic weighing, precise force measurement, inertial navigation, and vibration measurement, especially for quick starting measurement field. Besides, the laser transducer can be used in measuring the refractive index and density of the transparent medium by putting the sample in one sub-cavity (S sub-cavity or P sub-cavity)[17,19], while the other sub-cavity serves as the reference sub-cavity. A higher resolution of the index and the density's measurement is expected with the use of the differential technique.

The authors wish to thank Tan Zhongqi for his help in reviewing and modifying this letter.

References

1. A. Abramovici, Z. Vager, and M. Weksler, J. Phys. E **19,** 182 (1986).
2. A. Abramovici, W. E. Althouse, R. W. P. Drever, Y. Gürsel, S. Kawamura, F. J. Raab, D. Shoemaker, L. Sievers, R. E. Spero, K. S. Thorne, R. E. Vogt, R. Weiss, S. E. Whitcomb, and M. E. Zucker, Science **256,** 325 (1992).
3. O. Jennrich, Class. Quantum Grav. **26,** 153001 (2009).
4. X. Ni, M. Wang, X. Chen, Y. Ge, and H. Rong, Meas. Sci. Technol. **17,** 2401 (2006).
5. J. Zhou, S. Dasgupta, H. Kobayashi, J. M. Wolff, H. E. Jackson, and J. T. Boyd, Opt. Eng. **40,** 598 (2001).
6. Z. Ying, F. Dejun, L. Zhiguo, G. Zhuanyun, D. Xiaoyi, K. S. Chiang, and B. C. B. Chu, IEEE Photonics Technol. Lett. **13,** 618 (2001).
7. W. B. Jr Spillman, Opt. Lett. **7,** 388 (1982).
8. S. Tai, K. Kyuma, and M. Nunoshita, Appl. Opt. **22,** 1771 (1983).
9. A. Wang, S. He, X. Fang, X. Jin, and J. Lin, J. Lightwave Technol. **10,** 1466 (1992).
10. D. V. Dao, K. Nakamura, T. T. Bui, and S. Sugiyama, Adv. Nat. Sci. **1,** 013001 (2010).
11. W. Holzapfel and W. Settgast, Appl. Opt. **28,** 4585 (1989).
12. W. Holzapfel and W. Settgast, Appl. Phys. B **49,** 169 (1989).
13. W. Holzapfel and M. Finnemann, Opt. Lett. **18,** 2062 (1993).
14. W. Holzapfel, S. Neuschaefer-Rube, and M. Kobusch, Measurement **28,** 277 (2000).
15. J. Ding, Q. Feng, L. Zhang, and S. Zhang, Appl. Opt. **47,** 5631 (2008).
16. C. Huang, Y. Li, and S. Zhang, Chinese J. Lasers (in Chinese) **30,** 501 (2003).
17. X. Long, G. Xiao, and B. Zhang, Acta Opt. Sin. (in Chinese) **30,** 3227 (2010).
18. V. G. Gudelev, A. Ch. Izmailov, and V. M. Yasinskii, Sov. J. Quantum Electron. **18,** 166 (1988).
19. W. Liang, Y. Huang, Y. Xu, R. K. Lee, and A. Yariv, Appl. Phys. Lett. **86,** 151122 (2005).